CrossMark

Life Assessment and Crack Growth Properties of Laser Cut Dual-Phase Steel

Daniel J. Thomas

Abstract The effect of laser cut-edges has been studied as a method for producing an optimum fatigue life performance of advanced high-strength steel. During this study, DP600 high-strength steel laser cut-edges have been fatigue tested under S-N and E-N fatigue loading regimes. The cut-edge surface characteristic properties and internal metallurgical alterations have been observed to directly influence fatigue life of the steel. This paper has investigated the crack initiation and growth properties of the initial crack to mode two. It is shown that alterations in the surface properties can be harnessed so that beneficial properties can be produced to retard crack initiation. It was determined that the laser power and cutting speed can be used independently to produce the appropriate balance between microstructure and optimum surface properties. Optimal fatigue lives were attained by minimizing the laser cut-edge surface damage, maintaining the formation of wide area striations and by forming a uniform layer of martensitic material close to the cut-edge. These results suggest that laser cutting can be used to enhance the fatigue life to failure of fracture-sensitive steel grades.

Keywords Laser processing · Laser cutting · Fatigue life · Crack growth

List of Symbols

A	Elongation to failure
AHSS	Advanced high-strength steel
E-N	Strain life
HAZ	Heat-affected zone
HCF	High cycle fatigue
H_v	Vickers hardness
kPa	Kilopascal
R_a	Arithmetic mean of departures from the mean line
R_q	RMS of the R_a
R_p	Maximum height of profile above the mean line
R_v	Maximum depth of profile below the mean line
R_t	Total $R_p - R_v$
S-N	Stress life
Wt	Weight

D. J. Thomas (✉)
College of Engineering, Swansea University, Bay Campus, Swansea, UK
e-mail: daniel.thomas@creationengineering.co.uk

Introduction

High strength steel grades are laser cut to produce a range of tailor welded blanks. These laser cut components can be utilized to produce adaptable cuts of any geometry and structure to manufacture a range of custom components [1]. By using the right laser cutting parameters that can bring about enhanced cut-edges and the ability to ensure flexible manufacture [2]. The point at which using optimum laser process parameters results in a small kerf width combined with the generation of only a narrow heat-affected zone (HAZ) [3]. The most critical laser cutting process parameters in order of importance are (1) laser power, (2) traverse cutting speed, (3) assist gas pressure, and (4) the assist gas type. It is these parameters that significantly influence cut-edge quality during the laser cutting process [4, 5].

Ideal laser cutting procedure parameters can generate blanks that have a 0.1 mm degree of tolerance [6–9]. When using optimum process settings, the cutting speed can be up to 5000 mm/min [10]. The temperature distribution is confined in the cut-edge surface layer and the laser energy

interaction at the workpiece surface is critical for forming the cut-edge microstructural properties [11–14]. Using high power intensity results in the beam being absorbed by the workpiece material, which can cause undesirable heating and vaporization of the workpiece material. Further problems such as workpiece distortion can also occur. The assist gas parameter interacts as a hydrodynamic process that melts the workpiece material and removes it through the bottom of the cut-edge. There are two types of assist gas used in laser cutting: reactive and non-reactive [15]. Reactive gases are used to cut low-alloy steels, in which the reactive gas such as oxygen creates heat, leading to increases the thickness that can be cut and/or the cutting speed. Non-reactive gases are delivered at higher pressures in order to exert the necessary momentum on the liquefied material [16].

Numerous research studies have been conducted to examine the effect of assist gas during the laser cutting process. Experimental results showed that the use of oxygen as an assist gas resulted in better quality cut-edges than when nitrogen and argon are used to cut stainless steel [17]. When cutting mild steel, oxygen assist gas cutting produces the best cut-edge quality [18]. The use of oxygen as an assist gas at low traverse cutting speeds results in the formation of a wavy cut-edge. The size and properties of the HAZ are also of importance due to the high potential for local degradation leading to embrittlement of the cut-edge. The increase of the kerf width further increases the size of striations formed on the cut-edge surface. Surface striations are primarily the cause for laser cut-edge roughness and are the paramount quality characteristic in laser cutting, and the formation of these features relates to both the cutting

process and workpiece properties [19–21]. Surface properties are as a result altered, which have an effect on the fatigue life performance of cut-edges. Ensuring that minimum surface and microstructural damage is incurred then fatigue life can be improved over the life of the parent material [22].

Experimental Methods

Material Properties

DP600 is a dual-phase Ferrite, Martensite, and Retained Austenite grain advanced high-strength steel (AHSS). The microstructure of this steel is shown in Fig. 1, and Table 1 presents the chemistry and mechanical properties.

Laser Processing

Laser cut-edges were generated using a Prima Industria Platino 1325 CO_2 laser. The cutting parameters used for generating laser cut-edges are shown in Table 2. For comparison, milled edges, denoted as 'smooth' in this study, were generated using a Hardinge VMC600II CNC milling machine.

Characterization

Surface micrographs of laser cut-edges were captured using a Leica optical light microscope. Microstructural characterization and HAZ size measurements were analyzed by observing the specimens traverse to the cut-edge.

Fig. 1 Microstructure of DP600 steels etched with 2% natal showing the Ferrite, Martensite, and Retained Austenite grain structure
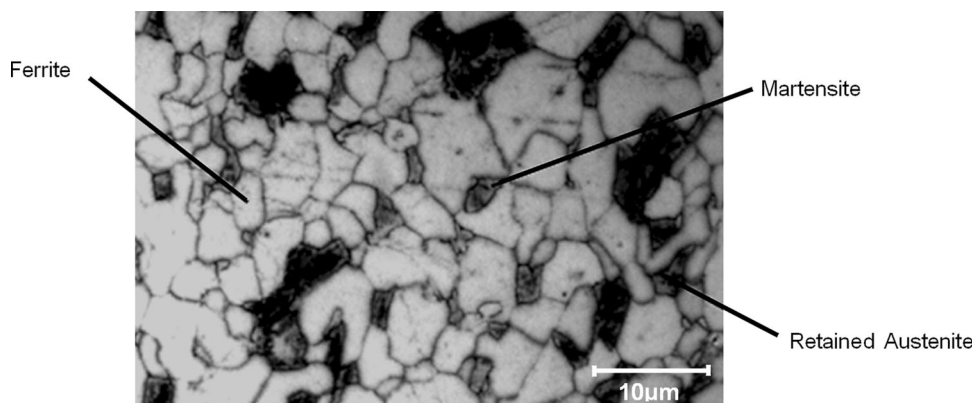
Table 1 Steel chemistry as a weight percentage and mechanical properties of DP600 steel grade

Element composition (%)							Mechanical properties			
C	Mn	Si	P	S	Al	Cr	Hardness (H_v)	Yield strength R_p (MPa)	Tensile strength R_m (MPa)	Elongation (%)
0.087	1.089	0.189	0.043	0.005	0.037	0.569	237	475.11	690.70	21.5

Table 2 The cut-edge process parameters used for generating laser cut-edges

Power (W)	Cutting speed (mm^{-1})	Assist gas	Pressure (kPa)	Head stand-off (mm)	Beam diameter (mm)	Lens (inches)	Focus height (mm)
800	1500	Oxygen/nitrogen	100	1.2	2.0	7.5	1.0
2000	1500	Oxygen/nitrogen	100	1.2	2.0	7.5	1.0
2000	4500	Oxygen/nitrogen	100	1.2	2.0	7.5	1.0

Metallographic analysis of the near-edge region microstructure was carried out by etching specimens using a 2% Nital reagent for 10 s. The microstructures were observed using a Reichert Polyvar optical microscope. In order to record and quantify cut-edge surface properties, a Taylor-Hobson form 2 Talysurf was employed with scans being carried out across a two-dimensional surface area, providing an accurate representation of the cut-edge roughness data parameters together with the generation of axonometric profiles. The degree to which the cut-edge surfaces had hardened was measured as Hardness Vickers (H_v) microhardness, and measurements were taken using a Leco M-400-G2 hardness tester with a 100-g load.
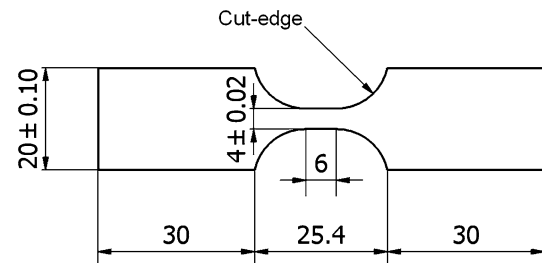
Fatigue Life Testing

Strain life (E-N) fatigue testing was conducted using an Instron 8516 with a 50 kN load cell and 30 kN hydraulic grips. The strain was controlled with a longitudinal extensometer. This testing was used to determine strain life to failure and cyclic stress/strain curves.

Stress life (S-N) fatigue testing was conducted using a Dartec 50 kN servo-hydraulic testing machine with a K7500 controller. All S-N life tests were carried out using a stress ratio of $R = -1$ at a frequency of 30 Hz. Stress life fatigue tests that ran to 1×10^7 cycles were considered to be run out tests. These fatigue data were compared with milled fatigue specimens denoted as smooth, which was used to determine the difference in the fatigue lives of cut-edges in comparison with smooth data. The semi-circle geometry of the fatigue specimen shown in Fig. 2 was cut using the laser process parameters detailed in Table 2, respectively, with the remainder of the specimen being polished.

Results

Cut-Edge Surface Characterization

Laser cut surfaces are have the surface appearance of a formation of striations. The nature of these formations is dependent on the applied process parameters and the properties of the material being cut. The three cut-edge

Fig. 2 Schematic of the fatigue specimen used for assessing E-N and S-N fatigue testing

types studied during this research are shown in Fig. 3. By comparing the cuts, it is clear to see that when using a high ratio of power to traverse cutting speed, there is an increase in melting with the formation of deeper striations as was the case when using 2000 W and 1.5 m/min. This is particularly because the high silicon content in the steel which reacts with the oxygen assist gas and increases the viscosity of the molten steel during the cutting process.

The periodic formation of surface striations produced when using high applied power was characteristically different with inconsistent striations produced. The surface roughness profiles of the laser cut-edges were observed to be only the slight formation of surface peaked features across the range of processing parameters. As the traverse cutting speed was increased, it was observed that the formation of striations at the bottom of the cut-edges became less pronounced. The striations became finer and closer together at the top of the cut-edge as the traverse cutting speed was increased because of increased focused energy interaction. As the laser power is increased, the striations became more distinctive because of the increased energy coupling. As the traverse cutting speed was increased to compensate, the striation became less distinctive. Observations signified that both the frequency and definition of surface striations are particularly apparent at high power settings.

Subsequently, a critical element for determining the striation pattern is the ratio between laser power and traverse cutting speed, with a higher ratio resulting in more power being delivered per unit area to the cut-edge. Additional power being absorbed into the material results in further disruptions and the generation of a coarse pattern of striations as the outcome.
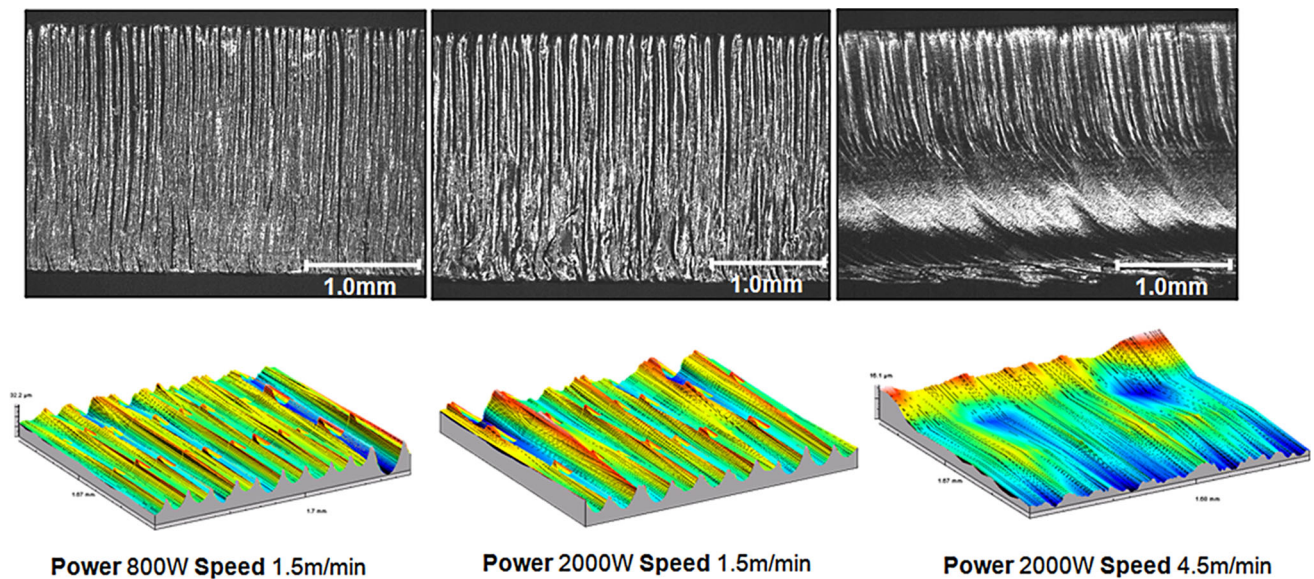
Fig. 3 Micrographs and axonometric profiles of DP600 laser cut-edge surfaces cut using each set of process parameters
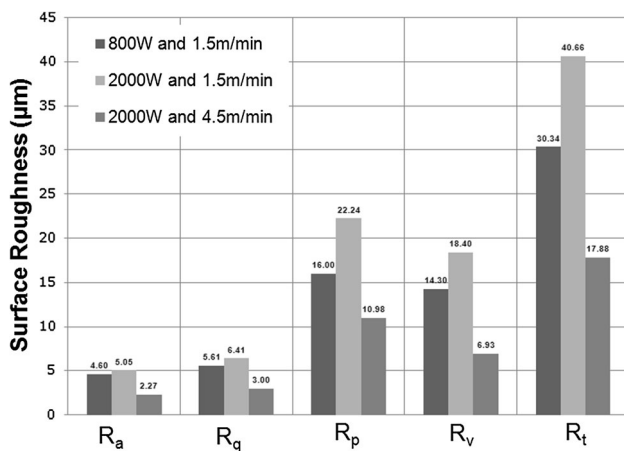
Fig. 4 Laser cut-edge surface roughness profiles showing the difference between the R_a, R_q, R_p, R_v, and R_t parameters formed using the different process parameters

Surface Topographical Characteristics

The properties of the surface striations when using different process parameters are shown in Fig. 4. Laser cut-edge surface roughness properties were observed to be directly influenced by the process parameters utilized. The R_a surface roughness parameters provide a good indication of your overall surface quality. As it can be seen, 2000 W 4.5 m/min process parameter resulted in the flattest surface. Further to this the 2000 W 1.5 m/min process parameters produce the roughest surface features. This is because as the power is increased, there is further power absorbed into the material and more melting of this material. As a result, the surface striations become larger as indicated by the significant increases in both the R_p and R_v parameters.

There was indeed observed to be a relationship between the shielding gas pressure and the level of surface melting. DP600 has a high level of silicon 0.189%, which reacts with the oxygen assist gas. As shown in Fig. 5, when nitrogen is used instead of oxygen, the surface profiles are completely different. As a result of the exothermic reaction, oxygen shielding gas increases the viscosity of the molten flow of liquid material and increased surface melting. This subsequently produces rougher patterns of striations.

Microstructural Properties

The internal microstructural properties of laser cut-edges generated using different process parameters are shown in Fig. 6. An inter-relationship between the cut-edge hardness and a thickness of the HAZ was recorded. Laser cut-edges generated using high power-to-traverse speed ratio resulted in harder cut-edge surfaces. It is due to the metallurgical alterations in the HAZ of the cut-edge that form a change in the measured transverse surface hardness. At 800 W, this resulted in the formation of comparably softer cut-edge surfaces.

The HAZ thickness is critical not only toward determining the quality of the cut-edge but also in ascertaining the depth of the metallurgical alterations that have occurred. It is the process of controlling the near-to-simultaneous heating, melting, and subsequent cooling process during laser cutting which is critical toward generating the minimum heat-affected damage to the workpiece. This occurs when using both a low power and low traverse cutting speed.

A fine transition boundary between the heat-affected material and the parent microstructure was found, as shown in Fig. 7. The region close to the cut-edge is phase transformed to martensitic material forming the HAZ. Martensite is a brittle microstructural phase structure and the transformation size and properties are controlled directly by the laser cutting process parameters.

Laser Cut-Edge S-N Fatigue Lives

The stress life (S-N) fatigue curves of the different laser cut-edges are shown in Fig. 8. It was observed that there was an improvement in the fatigue life under high stress for cut-edges generated using 2000 W and 1.5 m/min process parameters (Fig. 8b). This was also the case for cut-edges generated using 2000 W and 1.5 m/min process parameters in which there was a slight increase in the fatigue life across the full range of stresses (Fig. 8a). This is particular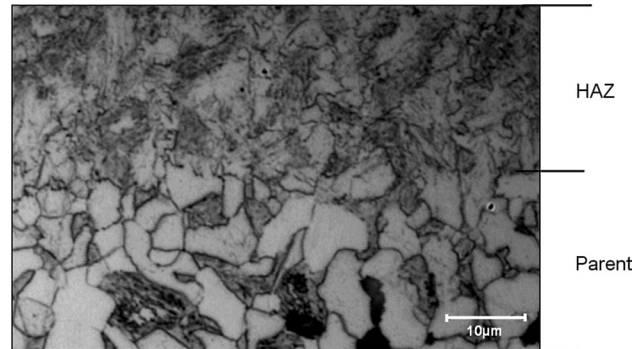ly seen under low stress loading which displayed a slight increase in fatigue life. However, when using 2000 W and 4.5 m/min process parameters, this resulted in a significant decrease in the fatigue life by a factor of 4.5 at an applied stress of 550 MPa (Fig. 8c).

Fig. 7 Optical micrographs of the HAZ transition region showing the microstructural change

Fig. 5 Surfaces of cut-edges using formed using 2000 W and 1.5 m/min using **a** oxygen and **b** nitrogen assist gases
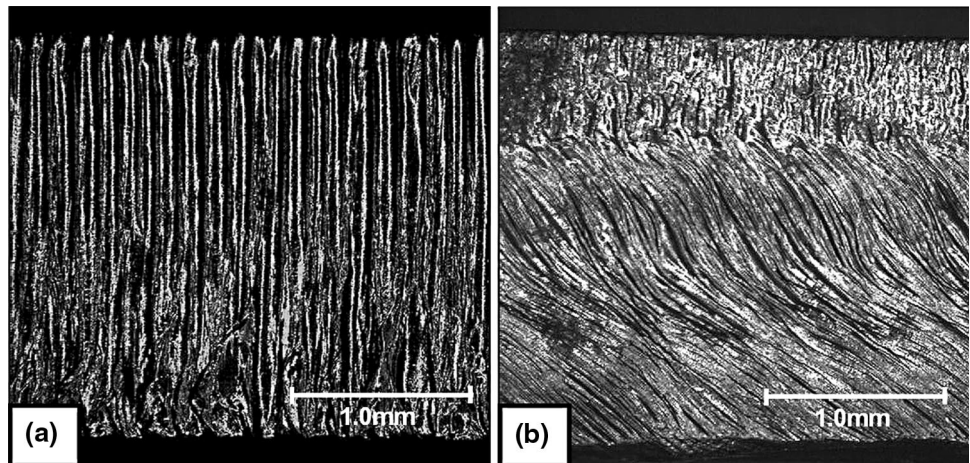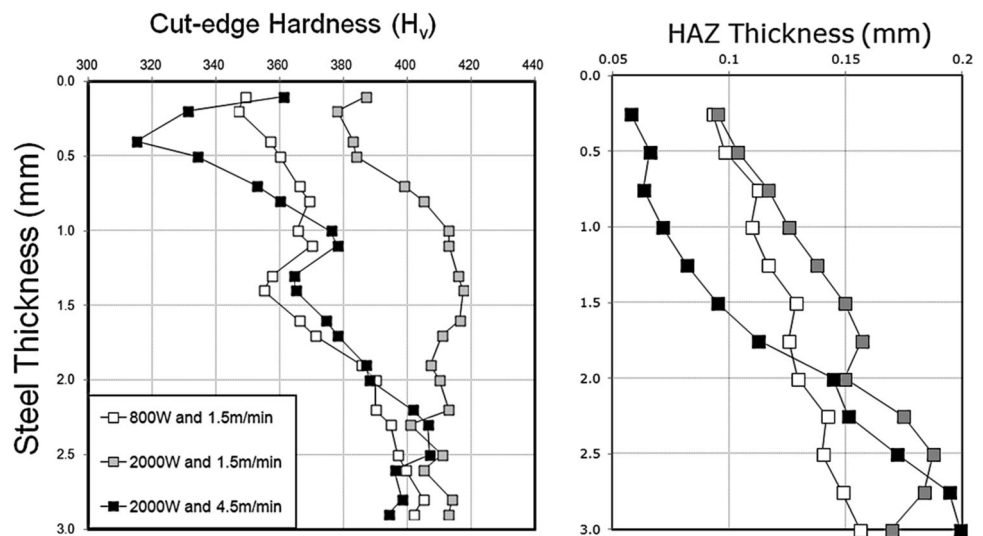

Fig. 6 Transverse surface hardness profiles 0.1 mm from the laser cut surfaces and the HAZ width through thickness of the cut-edges

The resulting crack formation appears brittle in characteristic and has resulted in rapid crack growth. Observations of the fatigue crack indicate that it started as a brittle initiation within the HAZ before propagating through to the more ductile parent microstructure. Observations of the crack propagation through the martensitic material of the HAZ were made as shown in Fig. 9. The region is critical to crack initiation because the properties of this phase transformation produced during the laser

cutting process can result in the generation of harder and more brittle cut-edge surfaces. It is these factors, which are also of significance toward the initiation mechanisms of the region I crack.
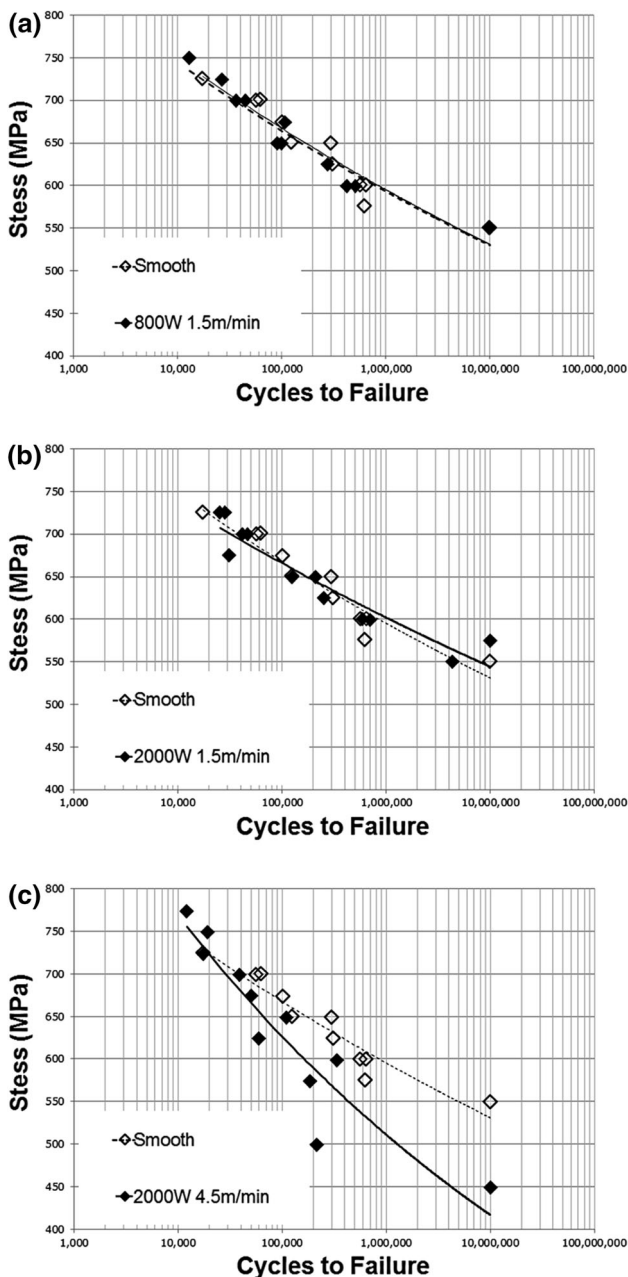
Laser Cut-Edge E-N Fatigue Lives

A fracture surface profile of the region I crack is shown in Fig. 10a, showing the smooth progression of the crack through the martensite heat-affected material. Micrographs of the crack initiation regions of laser cut-edges subtly show that the fatigue crack initiates at the apex of a surface striation as evidenced in Fig. 10b.

The comparison of strain life fatigue curves of smooth with the optimum laser cut-edge, using 800 W and 1.5 m/min process parameters of DP600, is shown in Fig. 11. It was observed that the strain life performance of laser cut-edges showed a slight decrease in performance over that of smooth edges. The extent and rate of cyclic softening under strain-controlled testing was evaluated.

Figure 12 shows the combined stress and strain comparison results of the fatigue lives of laser cut-edges. These results show significant variability of fatigue life performance. These show an improvement over that of smooth edges. Under cyclical deformation, the one single reversal of inelastic strain can change the stress-strain behavior of the steel. The mechanisms of microstructural hardening and softening are therefore a key factor. Changes in cyclic deformation behavior are more pronounced at the beginning of cyclic loading due to transient behavior.

Under closer examination, it was identified that DP600 had the formation of multiple fatigue cracks as shown in Fig. 13. These were observed to be independent of the primary crack which, propagated from the cut-edge surface. These properties are again interesting as it shows the
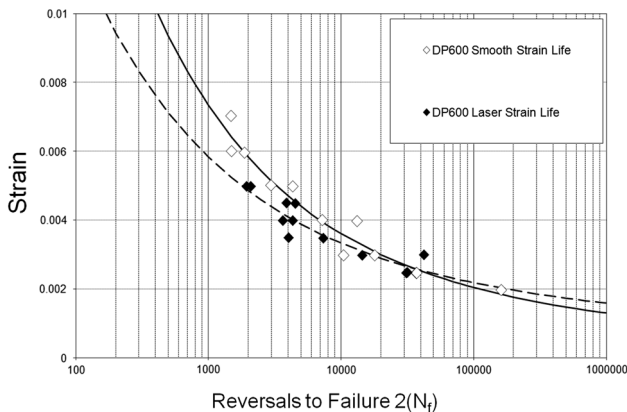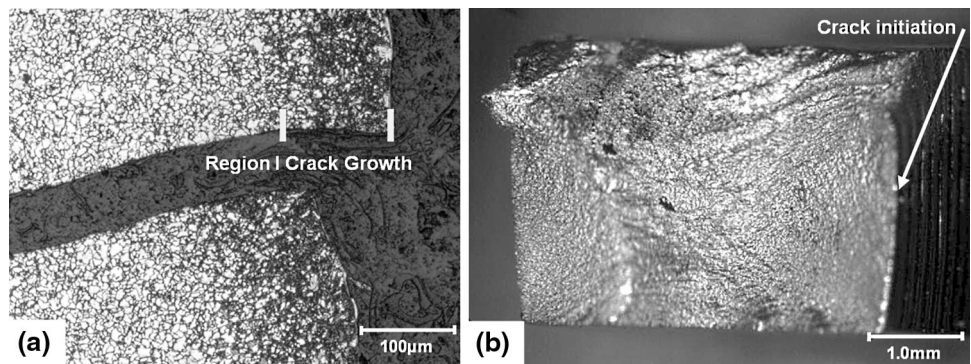
Fig. 8 S-N fatigue curves of DP600 laser cut-edges in comparison with smooth edges using **a** 800 W and 1.5 m/min **b** 2000 W and 1.5 m/min and **c** 2000 W, and 4.5 m/min
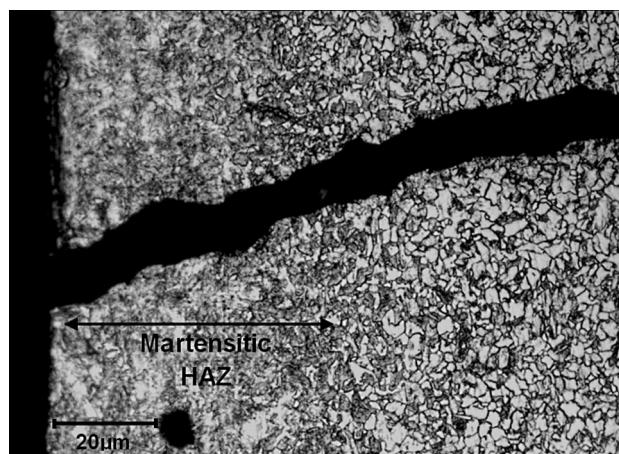
Fig. 9 The crack initiation of DP600 through a laser cut-edge martensitic heat-affected zone

Fig. 10 Crack initiation **a** microstructural micrograph of a crack initiation and **b** traverse profile of the fracture surface

Fig. 11 E-N fatigue curves of DP600 smooth edges in comparison with laser cut-edges generated using 800 W and 1.5 m/min cutting process parameters

Fig. 12 Stress life vs strain life of DP600 smooth edges in comparison with laser cut-edges generated using 800 W and 1.5 m/min cutting process parameters
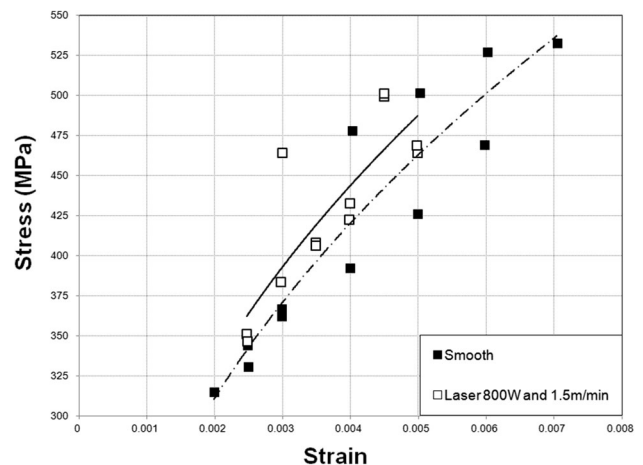
formation of subsequent non-conventional fatigue crack growth. Crack growth was observed to grow 90° to primary crack growth.

Strain life initiation of a laser cut-edge fatigue crack is shown in Fig. 14, showing that under a strain life test, the crack initiates at the trough of a striation. However, the crack was observed to also grow over the peak of a striation and move through an adjacent striation trough.
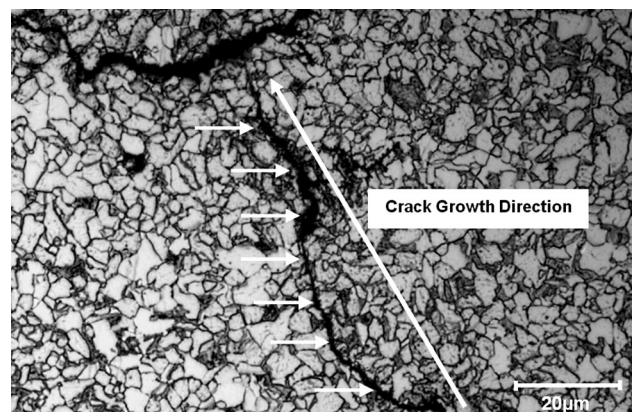
Under higher magnification examination, it was identified that the crack was inter-granular in nature. It is the crack growth properties that are critical toward understanding the ultimate failure of the steel grade. During the first phase of fatigue crack growth, the near-edge microstructural is critical toward the propagation. Therefore, although there are stress-raising striations features in the near edge region, it is these microstructural deformations that are critical towards retarding fatigue crack growth.

Discussion

DP600 has been selected for study during this investigation because of its increasing tendency toward fatigue life

Fig. 13 Internal brittle inter-granular crack growth propagation observed through the DP600 microstructure

sensitivity [20]. Previous studies have shown [21] that advanced high-strength steels have an increased sensitivity to fatigue due to their chemistry and microstructural properties. This is why laser cutting has been investigated as a method toward reducing the sensitivity of fatigue crack
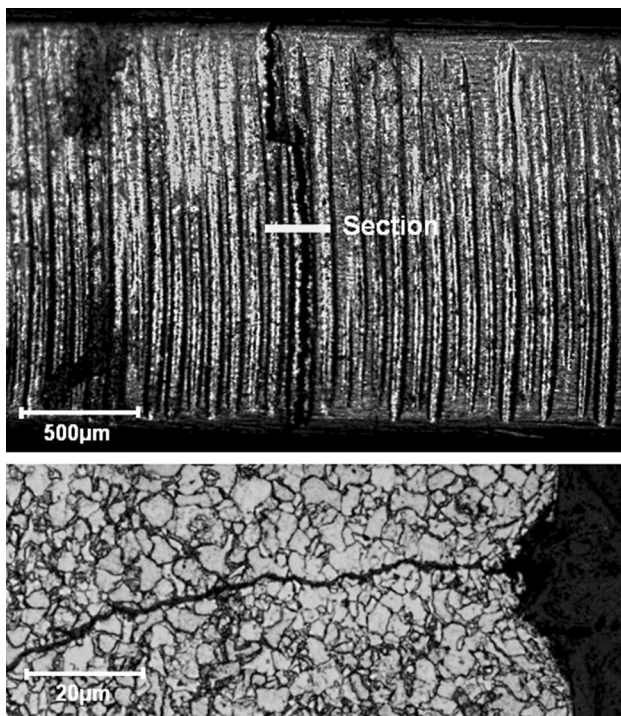
Fig. 14 Micrographs of the initiation of a laser cut-edge under strain life testing. Showing the fatigue crack initiating from the trough of a striation and the growth through the steel microstructure

formation. The chemistry properties of DP600 steel listed in Table 1 includes high concentrations of chromium and manganese. The inclusion of these two elements has the effect of increasing the steel hardness. The microstructural formations of the tri-phase structure which consists of martensite, ferrite, and austenite phases are shown in Fig. 1.

In the present work, laser cut-edges have been found to have a significant influence on the mechanical properties, including hardness and topographical, as shown in Figs. 3, 4, and 6. These properties have been shown to have actively been controlled by alterations in the laser process parameters. Slight alterations in a power and traverse cutting speed have produced a range of cut-edge qualities.

Critically, the effects of laser power, cutting speed, and the resulting energy coupling factor on the cut-edge have been investigated. It is found that increasing laser power and subsequent energy coupling factor increase both the surface roughness and also the surface hardness properties. The surface produced during the laser cutting process has the formation of a pattern of striations. These are shown in Fig. 3 in the form of overlaps of molten steel which are deposited behind the laser beam. Studying these using 3D axonometric profiling has provided an indication toward achieving optimum laser cut surfaces. The surface striation features produced are heavily dependent on the chemistry

of the steel and the reaction with the assist gas. The high silicon content of DP600 reacts with the oxygen shielding gas and increases the viscosity of the molten steel. This is less pronounced when using nitrogen shielding gas which is inert as shown in Fig. 5. The measured optimum surface roughness properties occurred when using 800 W of power at a 1.5 m/min^{-1} traverse cutting speed. Harder cut-edge surfaces were produced when the ratio between laser power to cutting speed was high in which additional laser power is absorbed into the cut-edge also producing a wider HAZ.

The evenness of the laser striations is of critical importance due to the fact that crack initiations were observed to propagate from the deepest feature. It is this region that acts as an intense stress raiser which also reduces fatigue life. Laser cut-edge strain life fatigue cracks were revealed to start at the trough of a striation, indicating that the properties of striations are important toward determining the fatigue life as shown in Fig. 10. Therefore, appropriate laser process parameters must be used to ensure that an even pattern of striations are produced.

The damaging properties of the HAZ can be minimized by matching the laser cutting speed with a proportional power level in order to produce a ductile cut-edge, which consists of an even pattern of surface striations. The properties of the HAZ are significant toward influencing fatigue life as shown in Fig. 9 where a fatigue crack has grown through the harder martensite HAZ. Further propagation of the fatigue crack subsequently grows into ductile parent microstructure. During the laser cutting process as a result of the phase transformation which forms martensite, there is subsequently a volume change in the crystalline structure of the steel. This subsequently forms increased compressive residual stresses due to phase changes in the material properties.

The influence of the laser cut-edge is more significant at low stresses and this is due to the fact that HCF properties depend strongly on surface characteristics as shown in Fig. 8. At a high number of cycles, striations formed during the laser cutting process act as a stress raiser. Subsequently, they are a source of localized plasticity and consequently crack initiation and initial crack growth.

When using optimum laser process parameters of 800 W and a traverse cutting speed of 1.5 m/min, cut-edges displayed fatigue lives equivalent to those of smooth edges. Figure 10 shows a fatigue crack which has formed at the trough of a laser striation, and therefore, it is critical to generate a near-flat surface during laser cutting to avoid stress being concentrated at a single large striation feature, which can result in a significant reduction in fatigue life.

It appeared that the internal properties of cut-edges provide the most important factor in controlled fatigue performance. In order to optimize the fatigue lives, process

parameters must be used which result in the generation of a HAZ, which is wide. The hard surface can be used to retard the initiation and initial growth of the fatigue crack. Minimizing the damaging effects of cut-edges in relation to fatigue life of DP600 can be achieved through the careful control of laser cutting process parameters.

Conclusions

The direct conclusions, which can be drawn from this work, include the following:

1. The fatigue response of cut-edges is highly dependent on the steel grade due to the mechanical, microstructural, and chemistry properties. This is critically the case of DP600 which has been shown to increase the sensitivity of the crack initiation and growth.
2. A relationship was identified between the width of the laser HAZ and the hardness of the cut-edge. It is the thickness of the HAZ that is affected by the laser process parameters which can be manipulated by adjusting the ratio between power and traverse cutting speed. Surface roughness properties provided an indication of the fatigue life of cut-edges.
3. The laser cutting process parameters used during this study have been determined to produce optimum fatigue performance comparable to that of smooth edges.
4. Laser cut-edges produced when using a power of 800 W and a traverse cutting speed of 1.5 m/min process parameters displayed the optimum fatigue performance for DP600.
5. These parameters resulted in the generation of a flat surface with less stress-raising features. This resulted in a distribution of stress area across the wide surface. It can, therefore, be recommended that the striation shape significantly influences the fatigue performance of laser cut-edges.
6. Provided that appropriate process parameters are used to generate laser cut-edges, slight improvements in fatigue life can be gained due to compressive residual stresses produced in the near-edge region.
7. This way the traverse cutting speed parameter can be adjusted to alter critical surface characteristics and microstructral properties in close proximity to the cut-edge.

References

1. S. Mullick, A.K. Agrawal, A.K. Nath, Effect of laser incidence angle on cut quality of 4 mm thick stainless steel sheet using fiber laser. Opt. Laser Technol. **81**(1), 168–179 (2016)
2. C. Wandera, A. Salminen, V. Kujanpaa, Inert gas cutting of thick-section stainless steel and medium-section aluminium using a high power fiber laser. J. Laser Appl. **21**(3), 154–161 (2009)
3. R. Poprawe, W. Schulz, R. Schmitt, Hydrodynamics of material removal by melt expulsion: perspectives of laser cutting and drilling. Phys. Proc. **5**(1), 1–18 (2010)
4. C. Wandera, V. Kujanpaa, Characterization of the melt removal rate in laser cutting of thick-section stainless steel. J. Laser Appl. **22**(2), 62–70 (2010)
5. L.D. Scintilla, L. Tricarico, A. Mahrle, A. Wetzig, E. Beyer, Experimental investigation on the cut front geometry in the inert gas laser fusion cutting with disk and CO_2 lasers. 30th International Congress on Applications of Lasers and Electro-Optics, ICALEO 2011, pp. 40–49 (2011)
6. D.J. Thomas, The influence of the laser and plasma traverse cutting speed process parameter on the cut-edge characteristics and durability of Yellow Goods vehicle applications. J. Manuf. Process. **13**(2), 120–132 (2011)
7. S. Cicero, T. García, J.A. Álvarez, A. Martín-Meizoso, J. Aldazabal, A. Bannister, A. Klimpel, Definition and validation of Eurocode 3 FAT classes for structural steels containing oxy-fuel, plasma and laser cut holes. Int. J. Fatigue **87**, 50–58 (2016)
8. J. Powell, D. Petring, R.V. Kumar, S.O. Al-Mashikhi, A.F.H. Kaplan, K.T. Voisey, Laser-oxygen cutting of mild steel: the thermodynamics of the oxidation reaction. J. Phys. D: Appl. Phys. **42**(1), Article No. 015504.
9. B.S. Yilbas, A.F.M. Arif, Laser cutting of steel and thermal stress development. Opt. Laser Technol. **43**(4), 830–837 (2011)
10. A. Lamikiz, L.N.L.D. Lacalle, J.A. Sánchez, D.D. Pozo, J.M. Etayo, J.M. López, CO_2 laser cutting of advanced high strength steels (AHSS). Appl. Surf. Sci. **242**(3–4), 362–368 (2005)
11. B.T. Rao, R. Kaul, P. Tiwari, A.K. Nath, Inert gas cutting of titanium sheet with pulsed mode CO_2 laser. Opt. Lasers Eng. **43**(12), 1330–1348 (2005)
12. J. Powell, S.O. Al-Mashikhi, A.F.H. Kaplan, K.T. Voisey, Fibre laser cutting of thin section mild steel: an explanation of the 'striation free' effect. Opt. Lasers Eng. **49**(8), 1069–1075 (2011)
13. A. Lara, I. Picas, D. Casellas, Effect of the cutting process on the fatigue behaviour of press hardened and high strength dual phase steels. J. Mater. Process. Technol. **213**(11), 1908–1919 (2013)
14. E. Nagels, J.R. Duflou, J. Van Humbeeck, The influence of sulphur content on the quality of laser cutting of steel. J. Mater. Process. Technol. **194**(1–3), 159–162 (2007)
15. B.S. Yilbas, C. Karatas, I. Uslan, O. Keles, Y. Usta, Z. Yilbas, M. Ahsan, Wedge cutting of mild steel by CO_2 laser and cut-quality assessment in relation to normal cutting. Opt. Lasers Eng. **46**(10), 777–784 (2008)
16. L.D. Scintilla, L. Tricarico, Estimating cutting front temperature difference in disk and CO_2 laser beam fusion cutting. Opt. Laser Technol. **44**(5), 1468–1479 (2012)
17. H.A. Eltawahni, M. Hagino, K.Y. Benyounis, T. Inoue, A.G. Olabi, Effect of CO_2 laser cutting process parameters on edge quality and operating cost of AISI316L. Opt. Laser Technol. **44**(4), 1068–1082 (2012)
18. L. Li, M. Sobih, P.L. Crouse, Striation-free laser cutting of mild steel sheets. CIRP Ann.: Manuf. Technol. **56**(1), 193–196 (2007)
19. K. Kheloufi, E.H. Amara, Numerical investigation of the effect of some parameters on temperature field and kerf width in laser cutting process. Phys. Proc. **39**, 872–880 (2012)

820

J Fail. Anal. and Preven. (2016) 16:811–820

20. A. Lamikiz, L.N. López de Lacalle, J.A. Sánchez, D. del Pozo, J.M. Etayo, J.M. López, CO_2 laser cutting of advanced high strength steels (AHSS). Appl. Surf. Sci. **242**(3–4), 362–368 (2005)

21. D.J. Thomas, M.T. Whittaker, G.W. Bright, Y. Gao, The influence of mechanical and CO_2 laser cut-edge characteristics on the fatigue life performance of high strength automotive steels. J. Mater. Process. Technol. **211**, 263–274 (2011)

22. D.J. Thomas, Finite element analysis of laser cut edge beam section for high stress intensity structural performance. J. Fail. Anal. Prev. **16**, 562–575 (2016)